Impulse-cyclone Drying Treatment of Poplar Wood Fibers and its Effect on Composite Material's Properties

Feng Chen,[a,b] Qingde Li,[a] Xun Gao,[a] Guangping Han [a] and Wanli Cheng,[a,*]

The fiber quality after a conventional drying treatment used for wood-plastic composites (WPCs) cannot be ascertained prior to use. Through the application of scanning electron microscopy, Fourier transform infrared spectroscopy, and X-ray diffraction, the effect of an impulse-cyclone drying (ICD) treatment on the quality of poplar wood fiber was first investigated. Subsequently, the effect of ICD conditions, such as inlet temperature, inlet wind velocity, and feed rate on the mechanical properties of WPCs and fiber dispersibility was considered. Also, the quality of fibers and WPCs was compared to those treated *via* an oven-drying method. Poplar wood fibers with a moisture content of 12.4% were pre-treated at different drying conditions by ICD. The obtained fibers were compounded with high-density polypropylene. The results showed that ICD could promote the hydration of poplar wood fibers and improve the mechanical properties of WPCs. The ICD-treated wood fibers were uniformly dispersed in the plastic matrix. With the increase of inlet temperature, the number of hydroxyl and carbonyl groups of poplar fibers decreased, whereas the degree of crystallinity increased as the inlet temperature and fiber meshes was increased. This study demonstrated the feasibility for the application of an ICD treatment in the WPCs production industry.

Keywords: Impulse-cyclone drying; Drying characteristics; Wood-plastic composites; Mechanical properties; Interfacial compatibility; Surface treatment; Poplar wood fiber

*Contact information: a: College of Material Science and Engineering, Northeast Forestry University, Harbin 150040, P.R. China; b: Liaoning Forestry Vocational-Technical College, Shenyang 110101, P.R. China; *Corresponding author: nefucwl@nefu.edu.cn*

INTRODUCTION

Derived from wood or agricultural materials, such as kenaf, jute, hemp, flax, or other natural resources, natural fibers have been widely used as reinforcing materials for plastics (Butylina *et al*. 2011). Water evaporation in natural fibers leads to the emergence of pores during the compounding process, which can result in inferior performances of wood-plastic composites (WPCs). Thus the natural fibers must be dry-treated, in advance, to a moisture content of 1% to 5% (Huang *et al*. 2006). After drying, the natural fibers can be prone to agglomeration, due to the formation of hydrogen bonds between cellulose molecules that contain many hydroxyl groups and thus cause uneven dispersion during mixing (Ndiaye *et al*. 2013; Pelaez-Samaniego *et al*. 2013; Effah *et al*. 2015). Moreover, the majority of polar (hydrophilic) natural fibers are not compatible with non-polar (hydrophobic) substances, due to the existence of many hydroxyl groups on the cellulose and hemicellulose of natural fibers. These circumstances can result in poor interfacial compatibility between the natural fibers and thermoplastics in WPCs (Shi *et al*. 2008; Sewda and Maiti 2013).

Wood fibers must be thoroughly dried to obtain good dispersion (Wang and Ying 2014). However, low dispersion, wood fibers agglomeration, and poor uniformity of the final moisture content still exist after drying, which reflects the reality of the WPCs industry. The commonly used drying treatments, such as rotary drum drying, oven drying, and flash drying, do not completely eliminate the stated deficiencies, which may not be appropriate for WPC production. In contrast, a number of researchers have studied hot air drying, impinging stream drying, flash tube drying, impulse drying, and other drying methods as pretreatments for wood particles or fibers in the production of particleboards and fiberboards. The WPC industry has more stringent requirements, such as lower moisture content, better uniformity, and better surface quality, than conventional wood composite production (Dang *et al.* 2008; Jarusombuti and Ayrilmis 2011). Few studies have examined the impact of a drying treatment on the quality of wood fibers, their dispersion in the plastic matrix, and the mechanical properties of WPCs. Therefore, a low-energy consumption, fast drying method, at a high temperature that provides a good dispersion to wood fibers will be one of the key technologies for WPC development.

More recently, researchers have focused on improving the drying techniques and satisfying the consumer demand for high-quality dried commodities (Liu *et al*. 2014). Applying the combined drying processes can pretreat commercial products, such as fiber, grain, or tablet for the medium-density fiberboard (MDF), medicine, food, chemical, and hospital industries. To reduce the disadvantages of hot air drying and preserve the final product quality, these processes include a mild pretreatment step (osmotic dehydration), hot air or solar drying, followed by microwave drying or another finishing drying method (Dev and Raghavan 2012). When compared with only one method, such as conventional drying, the synergistic and additive effect of two drying stages allows for the preparation of the products with a higher quality

Because an impulse drier may remove the free water and part of the bound water through acceleration and deceleration alternating with tube diameter variations and an increase in the mass transfer efficiency, impulse drying has been the most common drying method in the MDF industry (Ribeiro and Costa 2008). Cyclone drying has been of great interest in the medical, chemical, and coal industries because of its ability to easily remove most bound water, due to the long residence time of material in the cyclone drier, which transfers heat to the interior of the material (Akpinar *et al.* 2003). The combination of impulse drying and cyclone drying may be used to overcome the disadvantages associated with the application of each method alone. The application of an impulse drier, followed by a cyclone drier, could reduce the costs, processing time, and obtain high-quality final products.

The objective of this study was to compare an impulse-cyclone drying (ICD) treatment with oven drying (OD) for WPCs. The effect of the different drying parameters on the drying quality, the dispersion of wood fibers in the plastic matrix, chemical composition, and the crystallinity of fibers was determined to obtain the final product that could be used in WPCs.

EXPERIMENTAL

Materials

Daqing Petrochemical Co., Ltd. (Heilongjiang, China) supplied the high-density polyethylene (HDPE 5000S resin, density 0.954g cm^{-3}, melt flow index 0.7 g/10 min, crystallinity percent 85%, and mol. wt. 3.0×10^5). Harbin Yongxu Wood-based Panel Co., Ltd. (Heilongjiang, China) supplied the poplar wood veneers with sizes ranging from 50 cm to 100 cm in length, 30 cm to 50 cm in width, and 0.4 cm to 0.6 cm in thickness. Using a wood fiber mill (FY600, Fuyang Energy Technology Co., Ltd., Xuzhou, China), the poplar wood veneers were smashed and milled into poplar wood fibers with particle sizes ranging from 20- to 40-meshes, 40- to 60-meshes, 60- to 80-meshes, 80- to 100-meshes, and 100- to 120-meshes. The length and diameter of fiber were measured by GE-5 high-definition digital microscope (Shanghai Longfa Optical Instrument Co., Ltd.). The different meshes of wood fibers were placed under the objective lens of the microscope which was adjusted to present the clear image. The wood fibers on the slide were measured for their length and diameter values through the measurement software of the microscope. 30 pieces of data were measured for each mesh segment and the average aspect ratio of the wood fibers was determined. The measured results of the fiber characteristics are shown in Table 1. Maleic anhydride-grafted polyethylene (MAPE), purchased from Guangzhou Bo Chen Co., Ltd. (Guangzhou, China), was used as the coupling agent between the wood fibers and the plastic matrix. Industrial paraffin wax, as lubricant, was also used for easy processing of the WPCs profile.

Table 1. Characteristics of Poplar Wood Fibers

Property Measured	20- to 40-Meshes*	40- to 60-Meshes*	60- to 80-Meshes*	80- to 100-Meshes*	100- to 120-Meshes*
Fiber Length (mm)	1.78 (±0.23)	1.53 (±0.18)	1.36 (±0.20)	0.94 (±0.16)	0.64 (±0.13)
Fiber Diameter (μm)	330 (±51)	283 (±35)	223 (±31)	192 (±47)	178 (±33)
Length-diam. Ratio	5.4 (±1.95)	5.4 (±1.61)	6.1 (±1.87)	4.9 (±1.44)	3.6 (±0.97)
MC at 23 °C (%)	12.4 (±0.19)				

Note: *The results are given as averages and standard deviations (in parentheses) from the mean values; MC- Moisture Content

Impulse-cyclone drying treatment of poplar wood fibers

Poplar wood fibers were dried with an ICD treatment device (MQG-50, Jianda Drying Equipment Co., Ltd., Changzhou, China). The functional diagram of the ICD treatment facility is shown in Fig. 1.

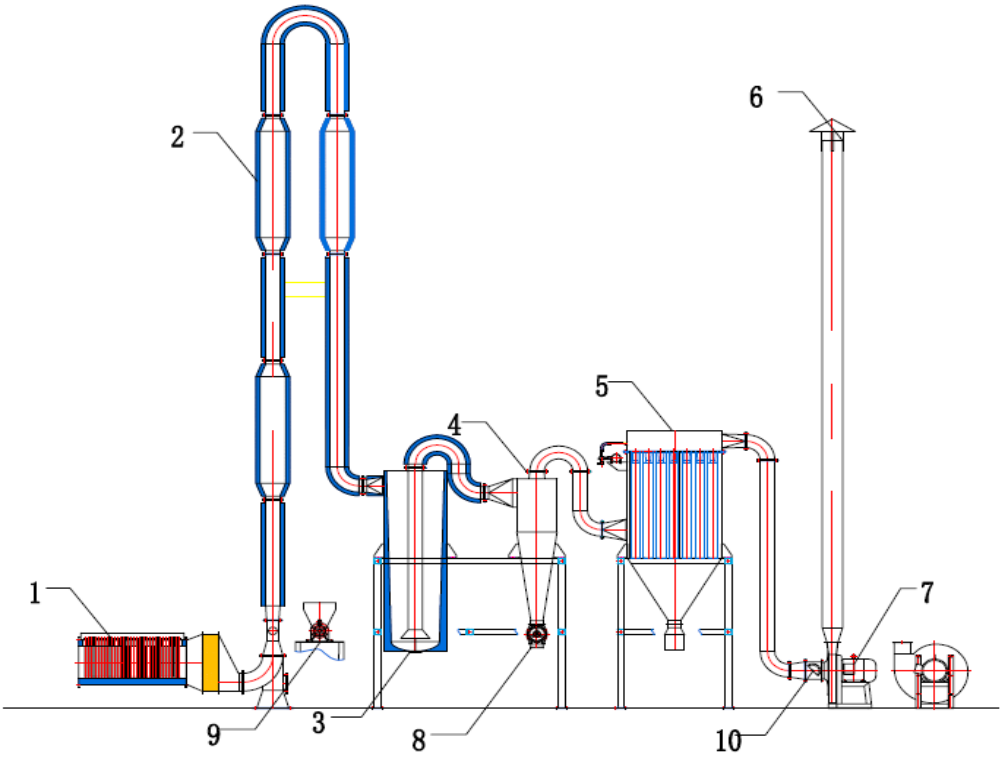

Fig. 1. Functional diagram of the ICD treatment facility: (1) Electric heater; (2) Impulse drier; (3) Cyclone drier; (4) Cyclone separator; (5) Dust collector; (6) Exhaust pipe; (7) Induced draft fan; (8) Air-off layout machine; (9) Screw feeder; and (10) Air valve

The experimental design for the ICD treatment was determined according to the required parameters in Table 2. The optimal condition for ICD was selected through preliminary tests. The poplar fibers dried at 103 °C ± 2 °C by an oven for 12 h were taken as a contrastive plot.

Table 2. Drying Parameters Design of ICD for the Poplar Fibers Samples

Drying Condition	Inlet Temperature (°C)	Inlet Wind Velocity (m/s)	Feed Rate (kg/h)	Fiber Size (mesh)
1	120	11	120	60 to 80
2	140	11	120	60 to 80
3	160	11	120	60 to 80
4	180	11	120	60 to 80
5	200	11	120	60 to 80
6	220	11	120	60 to 80
7	240	11	120	60 to 80
8	200	7	120	60 to 80
9	200	8	120	60 to 80
11	200	10	120	60 to 80
12	200	11	120	60 to 80
13	200	12	120	60 to 80
14	200	13	120	60 to 80
15	200	11	60	60 to 80

16	200	11	75	60 to 80
17	200	11	90	60 to 80
18	200	11	105	60 to 80
19	200	11	120	60 to 80
20	200	11	135	60 to 80
21	200	11	150	60 to 80
22	200	11	120	20 to 40
23	200	11	120	40 to 60
24	200	11	120	60 to 80
25	200	11	120	80 to 100
26	200	11	120	100 to 120

Preparation of wood fiber/HDPE composites

Wood fibers (50 wt.%), HDPE (45 wt.%), MAPE (3 wt.%), and paraffin (2 wt.%) were mixed and stirred in a high-speed mixer. The resultant uniform mixture was then placed into an SJSH30/SJ45 two-stage plastic extruder (Nanjing Rubber & Plastic Mechanic Co., Ltd., Nanjing, China).

After granulation and extrusion molding, the standard specimens were prepared for impact, flexural, and tensile testing. There were six specimens with the dimensions of 80 mm × 10 mm × 4 mm (impact tests), 80 mm × 13 mm × 4 mm (flexural tests), and 165 mm × 20 mm × 4 mm (tensile tests) in each group.

Methods

Fiber drying quality analysis-moisture content

The final moisture content and dehydration content of fibers were tested according to Chinese National Standard GB/T 1931 (2009). The sample after an ICD or OD treatment was weighed and placed in the oven. The oven temperature was set at 103 °C ± 2 °C with a drying time of 8 h. The mass was measured once every two hours. When the mass change was less than 0.002 g, the absolute drying status of the fibers was determined. Equation 1 was used to measure the absolute moisture content, which was accurate to 0.1 g,

$$W(\%) = \frac{m_1 - m_0}{m_0} \times 100 \quad (1)$$

where W is the moisture content of the sample (%), m_1 is the sample mass (g) before testing, and m_0 is the absolute dry mass of the sample (g). The final measurements were obtained by calculating the arithmetic mean of the five specimens.

Surface quality

By using a SEM-EDXA Scanning Electron Microscope (SEM) (FEI Company, Eindhoven, Netherlands), the surface quality of the fibers was analyzed to observe the wood fiber breakage and roughness degree during stirring and mixing. Before the observation, the samples were coated with platinum (Pt) to improve the surface conductivity and then observed at an acceleration voltage of 15 kV. A zoom range of 50x to 600x was selected for the observation.

Characterization of Wood Fibers

FTIR procedure and analysis

Using the KBr disc technique (1 mg of sample powder/300 mg of KBr), the FTIR measurement was performed with a Nicolet Nexus 6700 FTIR spectrometer (American Thermo Fisher Scientific company, Waltham, USA) at a resolution of 4 cm^{-1}, 32x scans, and a scanning range of 4000 cm^{-1} to 600 cm^{-1}. Three replicate measurements were recorded for each condition.

Wide-angle X-ray Diffraction (WXRD)

A D/MAX 2200 X-ray diffractometer (Rigaku Corporation, Tokyo, Japan) was used to measure the WXRD patterns of the fiber samples before and after modification. Prior to the measurement, the samples were placed onto the supporter and pressed compactly. Over the angular range of $2\theta = 5°$ to 40° and a step size of 5°/min, the WXRD data were generated by a diffractometer with Cu Kα radiation (λ = 1.542 Å) at 40 kV and 30 mA. The degree of crystallinity, or crystallinity index (CI%), was evaluated for each sample using Eq. 2,

$$CI = (A_c / A_a) \times 100\% \quad (2)$$

where A_c is the area of the crystalline reflection and A_a is the area subtending the whole diffraction profile. PMGR program (Rigaku Corporation, Tokyo, Japan) of the instrument was used to test and export the data. The WXRD jade software (MDI JADE 6.5, Materials Data, Inc., Livermore, California, USA) was adopted to calculate the diffraction peaks (002), the crystalline reflection, and the area subtending the whole diffraction profile. Three parallel experiments were performed in the test and the arithmetic mean of the three measurements was taken as the experimental result.

Mechanical measurement of WPCs

The specimens with the typical dimensions of 80 mm × 13 mm × 4 mm for flexural testing were measured under the three-point bending test using an RGT-20A electronic mechanics testing machine (Shenzhen REGER Instruments Co., Ltd., Shenzhen, China) in accordance with Chinese National Standard GB/T9341 (2000). A crosshead speed of 5 mm/min and a span length of 64 mm were used for the test. Tensile testing was conducted from specimens with a dimension of 165 mm × 20 mm × 4 mm using the same Universal Testing Machine according to Chinese National Standard GB/T1040 (1992). A crosshead speed of 10 mm/min and a gage length of 64 mm were used for the test. The impact strength was determined from specimens with a dimension of 80 mm × 10 mm × 4 mm using a XJ-50G impact tester (Chengde Precision Testing Machine Co., Ltd., Chengde, China) according to Chinese National Standard GB/T1043 (1993). Five replicate specimens were taken for each test and the average data along with corresponding standard deviations were reported.

Dispersibility analysis

The dispersibility of fibers and their composites were observed under a SEM-EDXA Scanning Electron Microscope (FEI Company, Eindhoven, Netherlands). The samples were taken from the tensile dumbbell test of WPCs. The samples were frozen in liquid nitrogen and fractured to obtain a well-defined fiber–matrix interface. The samples were spray-coated with gold prior to the observation to enhance the surface conductivity,

and observed under SEM at an acceleration voltage of 15 Kv A biological microscope (Changfang Optical Instrument Co., Ltd., Shanghai, China) with a 4x target lens. The dried fibers were agitated using a high-speed mixer. A 200 mL beaker was used to sample poplar fibers from the mixer outlet, and then 20 g of the fibers in the beaker were naturally poured onto a 100 mm diameter slide to observe under the biological microscope.

RESULTS AND DISCUSSION

Fiber Drying Quality Analysis

Moisture content analysis

In Fig. 2, the final moisture content and dehydration content of wood fibers are shown as a function of the inlet temperature, inlet air velocity, and feed rate. The end moisture content of poplar wood fibers was found to decrease with the increase of ICD inlet temperature. High-temperature had the ability to increase the internal and external temperature and moisture gradient on the surface of fibers, which was conductive to the superficial vaporization of wood fibers and water molecular movements from wood fibers.

In contrast, the end moisture content of poplar wood fibers was found to increase with the increase of inlet air velocity and feed rate. The low inlet air velocity increased the staying time of the fibers in the cyclone drier, which increased the heat and mass transfer between the airflow and the fibers. A high feed rate increased the charging frequency and collision chance of wood fibers, which reduced the staying time in the wood fiber drier and weakened the heat and mass transfer between the wood fibers and airflow. In addition, the total evaporation capacity of the fiber moisture increased and the airflow temperature decreased. Therefore, the heat and mass transfer capacity of the whole drying system decreased and the mass transfer content slowed down.

The variable coefficient of the moisture content with an OD treatment as the untreated sample was high and some fibers were too dry, which could have resulted in fracture when the fiber was mixed with the plastic. When compared with OD (12 h), the drying time of ICD was 16 s to 30 s, and the final moisture content of the fibers was more easily decreased to the even state.

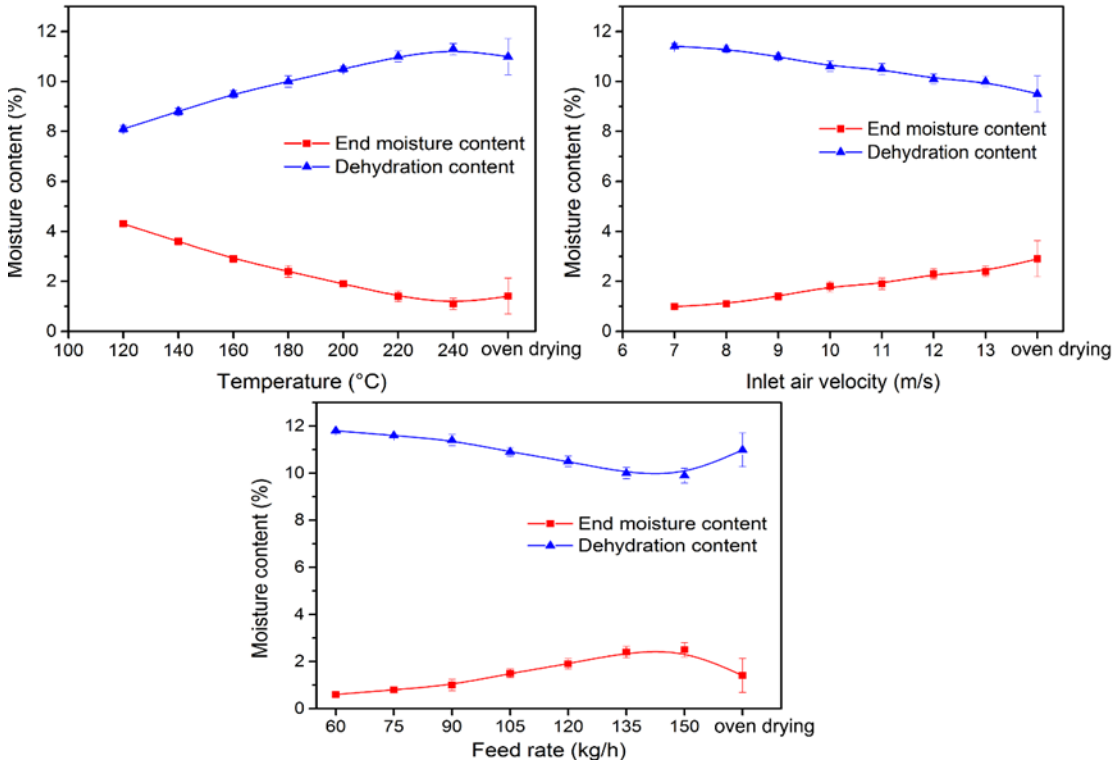

Fig. 2. Effect on moisture content and dehydration content with different drying parameters

Surface quality analysis

After stirring with a high-speed mixer, the surface SEM morphology of dried poplar wood fibers is shown in Fig. 3. Figure 3(a) is the fiber surface observed in the SEM image with ICD treatments.

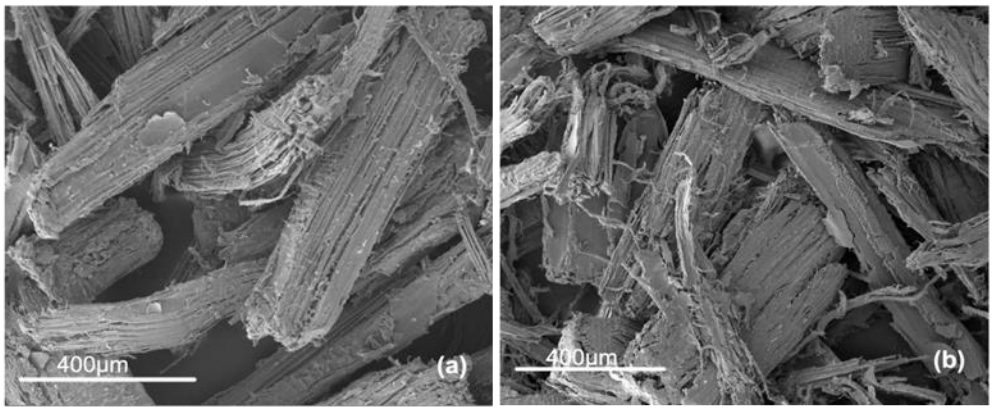

Fig. 3. SEM morphology of poplar fiber surface quality after stirring; (a) ICD treatment, T = 200 °C, F = 120 kg/h, V = 11 m/s, M = 60 to 80 meshes; and (b) OD treatment

Wood fibers were shattered and crushed less, indicating that wood fibers have good mobility in the molten state of HDPE, which is conductive to dispersity of wood fibers in the resin matrix (Harper and Wolcott 2004). To some extent, it avoids agglomeration of wood fibers, and thus it improved the overall performances of WPCs. Figure 3(b) is the fiber surface observed in the SEM image with an OD treatment. Multiple breakages were

observed on the surface of the fibers, which indicated that the brittleness of the wood fibers increased after OD treatment and fracture occurred during stirring and mixing. Therefore, the mechanical properties of the OD-treated fibers and the resultant composites could decrease.

FTIR Analysis

The FTIR spectra attribution results are shown in Table 3. The main absorption peak in FTIR was 3350 cm^{-1}, the O-H stretching vibration was 2890 cm^{-1}, the C-H stretching vibration (aliphatic series) was 1730 cm^{-1}, the C=O stretching vibration (xylan) was 1600 cm^{-1}, the benzene ring carbon skeleton stretching vibration (lignin) was at 1240 cm^{-1}, and the benzene-oxygen bond stretching vibration (lignin) and acyl-oxygen bond (CO-OR) stretching vibration (hemicellulose) was at 1030 cm^{-1}.

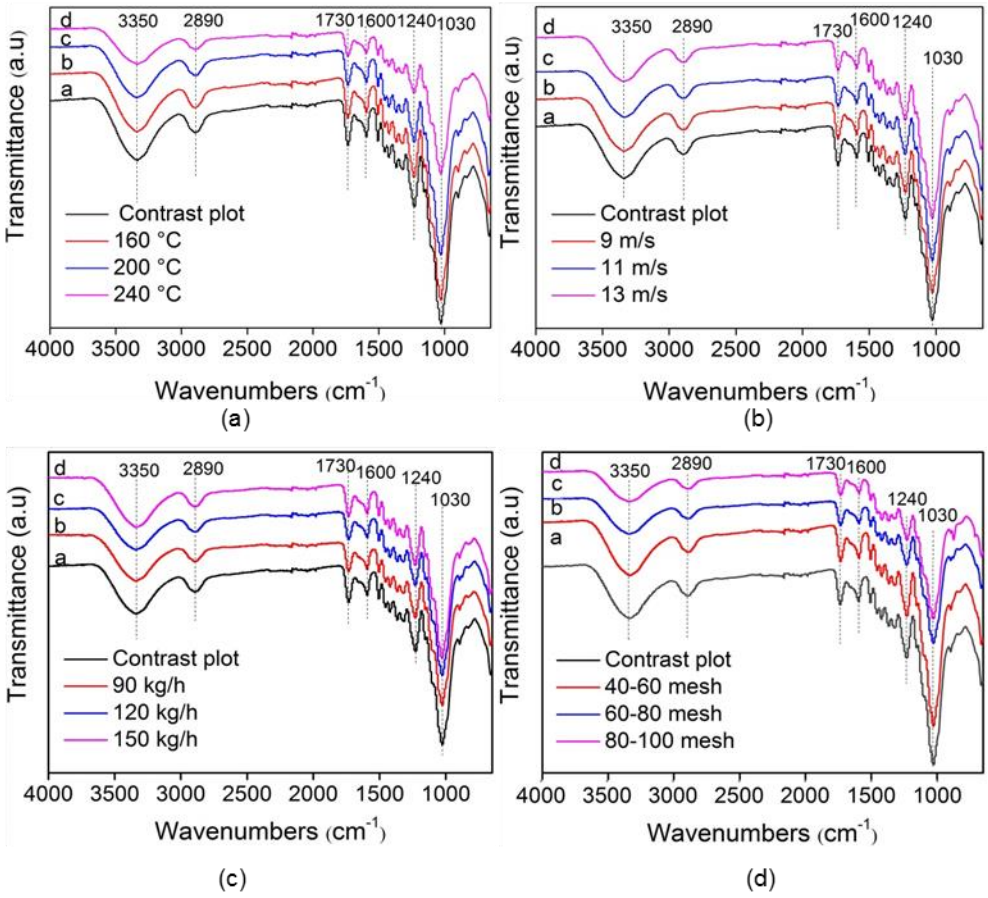

Fig. 4. Comparison of FTIR spectra obtained for poplar wood fibers by OD and ICD treatments under different drying conditions; (a) Inlet temperature; (b) Inlet air velocity; (c) Feed rate; and (d) Fiber size

Table 3. FTIR Spectra Attribution of Absorbance Bands

Wavenumber (cm^{-1})	Spectra Attribution
3350	Hydroxyl (-OH) stretching vibration
2890	Methyl ($-CH_3$), methylene ($-CH_2$) stretching vibration
1730	Carbonyl (C=O) stretching vibration (xylan)
1600	Benzene ring carbon skeleton stretching (lignin)
1240	Benzene-oxygen bond stretching vibration (lignin); acyl-oxygen bond (CO-OR) stretching vibration (hemicellulose)
1030	Secondary alcohols and aromatic ether (C-O) stretching vibration (cellulose, hemicellulose, and lignin)

Figure 4 shows the comparison of the FTIR spectra obtained for poplar wood fibers by OD and ICD treatments under different drying conditions. The ICD treatment showed little impact on the chemical composition of poplar wood fiber, while it had a large impact on the absorption intensity of functional groups. Compared with the unmodified samples, the absorption intensity of the characteristic peaks of the samples treated under 160 °C did not change noticeably. However, the absorption intensity of the -OH stretching vibration peak at 3350 cm^{-1} decreased slightly with the increase of the inlet temperature of the ICD treatment. This indicated that the number of free hydroxyl groups decreased with higher temperatures. As the inlet temperature increased, the adsorption intensity of methyl ($-CH_3$) and methylene ($-CH_2$) stretching vibration peaks around 2890 cm^{-1} also decreased. This result revealed that a higher temperature accelerated the molecules' decomposition and esterification within the fiber. The peak at 1730 cm^{-1} was attributed to the stretching vibration of the non-conjugated carbonyl group (C=O) of xylan, which was the main characteristic peak of hemicellulose and different from other components. With the increase of temperature, the adsorption intensity of the C=O stretching vibration peak decreased, which showed that the higher temperature and moist environment in hot air could make the acetyl group hydrolyze into acetic acid and reduce the number of hydrophilic C=O functional groups. The peaks around 1600 cm^{-1} were attributed to the carbon skeleton vibration of benzene rings, which were the characteristic absorption peaks of lignin. For the sample treated at 160 °C and 200 °C, the intensity did not vary much. However, the intensity was reduced significantly at 240 °C, which indicated that the lignin in fiber had decomposed below 240 °C. The peaks around 1240 cm^{-1} were the characteristic absorption peaks of hemicellulose and lignin. These peaks diminished gradually as the temperature increased, which indicated that higher temperatures could promote hemicellulose deacetylation and ultimately decompose it into monosaccharides.

Figure 4(b) shows the effect of different airflow drying conditions on the characteristic absorption peak strength in the fiber. The -OH stretching vibration peak at the 3350 cm^{-1} band, the C-H stretching vibration absorption peak at the 2890 cm^{-1} band, and the C=O stretch movement peak and the C-O stretch peak's absorption strength at the 1730 cm^{-1} band all revealed a decreasing tendency with the reduction of drying airflow. However, the influence on the C=O stretch vibration characteristic peak strength at the 1600 cm^{-1} band was minimal. This indicated that the number of hydroxyl and carbonyl groups in the wood fiber could be reduced slightly with the decrease of airflow and long stay of materials in the drier. The impact different airflow drying on lignin was limited.

Figure 4(c) shows the FTIR spectra of poplar fibers on the condition of different feed rates. It was observed that the variation of the absorption strength for the characteristic peaks was small with different feed rates of 150 kg/h and 90 kg/h. When the feed rate was 120 kg/h, the -OH stretching vibration peak, the C-H stretching vibration absorption peak, wave number C=O stretching movement peak, and the C-O stretching peak absorption strength had clearly fallen, which indicated that the influence of 150 kg/h and 90 kg/h feed rates on the wood fiber's functional group was minimal. This result was due to the fact that the carrier tape rate of wood fiber in the airflow was low at a low feed speed, which made the fiber easy to move quickly with the airflow. The shorter the stays in the drier were, the less noticeable that the functional groups change was. At a high feed speed, the carrier tape rate of the wood fiber was high in the airflow. The collision and friction of material to material from the cyclone cavity increased. Therefore, the materials are easily taken out by the airflow. In addition, the retention time was short and the absorption strength change in the functional group of the wood fiber was small as well.

Figure 4(d) shows the FTIR spectra of poplar fibers with different mesh sizes after impulse-cyclone combined drying. As observed, the -OH stretching vibration peak, C-H stretching vibration absorption peak, C=O stretching movement peak, and C-O stretching peak all showed a decreasing absorption strength with the decrease of fiber mesh. This was due to the larger materials' particle size, and the larger mass with the longer materials' stay in the airflow. Furthermore, the decreased degree of the absorption peak strength for hydroxyl, carbonyl, and other official groups in the fiber was more noticeable.

Wide-angle X-ray Diffraction (WXRD)

The crystallinity of wood materials was one of the primary factors that affected the mechanical properties. Figure 5 illustrates the WXRD patterns obtained for the untreated and modified wood fibers. As shown in Fig. 5, the (002) diffraction peaks recorded for the untreated and modified wood fibers were both centered at approximately 22° (ranging from 21.32° to 22.88°). This result indicated that the modification process resulted in a limited change of the crystalline regions of wood fibers and the minimal effect on the distance between crystal layers. However, the modification process had a profound impact on the crystallinity of wood fibers.

As shown in Fig. 5(a), the crystallinity of poplar wood fibers with ICD increased from 50.79% to 66.18%, which was higher than that with OD. The result indicated that increasing the ICD inlet temperature had a stronger impact on the amorphous region of the fiber. This could have been due to the fact that through the ICD treatment, the "bridging reaction" between the hydroxyl groups of microfibrils in the amorphous region occurred, the hydroxyl groups dehydrated and formed eternal bonds, microfibrils were arranged in the amorphous region, and the crystallinity of cellulose was then increased. When the inlet temperature was 240 °C, the hemicellulose of poplar fiber could hydrolyze in the steam of hot air to form acetic acid. The acetic acid that formed degraded the microfibrils in the amorphous and crystalline regions and hydrolyzed the glucose unit into short chain structures, which led to a lower crystallinity of cellulose in poplar wood fiber under this temperature condition.

As shown in Fig. 5(b), the crystallinity of the dried specimen cellulose increased from 52.6% to 66.4% with the increase of inlet wind velocity. When the inlet wind velocity was lower, the retention time of the poplar fiber in the drier increased, which led to the degradation of microfibers in the non-crystallizing area of cellulose, and thus the relative crystallinity of cellulose decreased.

As shown in Fig. 5(c), the cellulose crystallinity was 46.4%, 66.2%, and 55.4% with the feed rate of 90 kg/h, 120 kg/h, and 150 kg/h, respectively. This indicated that the medium feed rates maximized the cellulose crystallinity. As shown in Fig. 5(d), the crystallinity of specimen cellulose was 55.5%, 66.2%, and 67.0% when the fiber form was 40 to 60 meshes, 60 to 80 meshes, and 80 to 100 meshes, respectively. With the increase of the fiber mesh number, the crystallinity of poplar fiber increased. This meant that with the reduction of the material mesh number, the larger and longer fiber sizes stayed in the drier and the microfiber had a higher degree of degradation. The relative crystallinity of cellulose showed a decreased tendency.

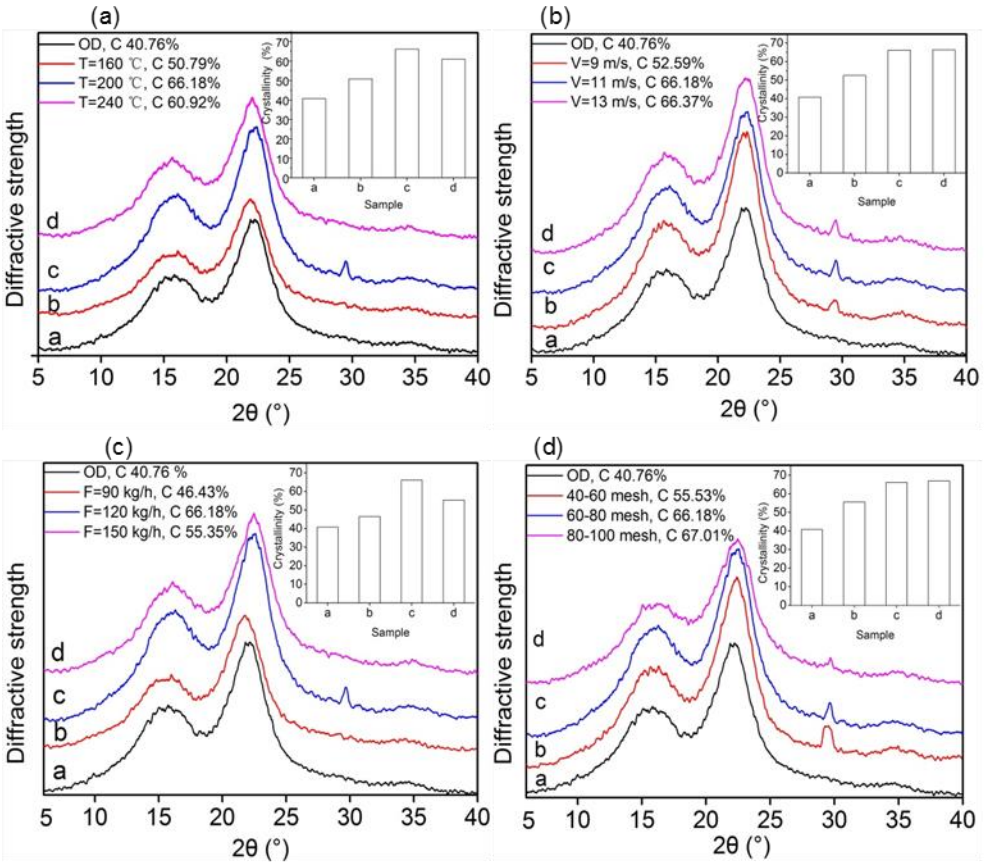

Fig. 5. XRD patterns obtained for poplar wood fibers by OD and ICD under different inlet temperatures (a), inlet air velocities (b), feed rates (c), and fiber sizes (d)

Effect of ICD Treatment on Mechanical Properties of WPCs

Table 4 shows the mechanical properties of WPCs at different drying conditions. The flexural strength, tensile strength, elasticity modulus, and impact strength of the composites with ICD-treated wood fibers were improved as the drying temperature increased from 160 °C to 220 °C. The modulus of elasticity reached the highest value at a temperature of 220 °C. The relative crystallinity of cellulose and the relative amount of lignin increased during the treatment due to the partial pyrolysis of hemicellulose, and thus the modulus of elasticity improved. Nevertheless, the flexural strength, modulus of elasticity, and impact strength decreased dramatically at 240 °C. This indicated that a further increase of temperature resulted in more pyrolysis inside the cellulose. The increase of the cellulose chain ruptures led to decreased mechanical properties.

Table 4. Mechanical Properties of WPCs by ICD and OD Treatment*

Drying Condition		Mechanical Properties of WPCs			
Variables of ICD Treatment	Inlet Temperature (°C)/Inlet Wind Velocity (m/s)/Feed Rate (kg/h)/Fiber Size (mesh)	Impact Strength ($kJ \cdot m^{-2}$)	Flexual Strength (MPa)	Modulus of Elasticity (GPa)	Tensile Strength (GPa)
Inlet Temp.	160/11/120/60~80	18.9 (0.52)	67.2 (0.75)	3.6 (0.06)	41.6 (0.39)
	180/11/120/60~80	20.3 (0.63)	73.7 (0.94)	3.9 (0.08)	41.6 (0.49)
	200/11/120/60~80	21.4 (0.25)	74.0 (0.59)	3.9 (0.06)	43.4 (0.69)
	220/11/120/60~80	22.7 (0.36)	75.9 (0.63)	4.3 (0.05)	43.6 (0.36)
	240/11/120/60~80	18.8 (0.41)	70.9 (0.64)	3.8 (0.04)	42.6 (0.53)
Inlet Wind Velocity	200/9/120/60~80	20.0 (0.67)	44.3 (1.38)	2.3 (0.13)	28.2 (1.21)
	200/10/120/60~80	20.6 (0.38)	59.9 (0.89)	3.1 (0.09)	32.2 (0.83)
	200/11/120/60~80	21.4 (0.25)	74.0 (0.59)	3.9 (0.06)	43.4 (0.69)
	200/12/120/60~80	21.2 (0.31)	67.2 (0.58)	3.6 (0.14)	40.0 (0.64)
	200/13/120/60~80	21.1 (0.31)	62.5 (0.65)	3.3 (0.06)	38.5 (0.79)
Feed Rate	200/13/90/60~80	19.2 (0.54)	68.0 (0.82)	3.8 (0.11)	41.1 (0.84)
	200/13/105/60~80	22.3 (0.46)	66.8 (0.87)	3.6 (0.05)	41.8 (0.79)
	200/13/120/60~80	21.4 (0.25)	74.0 (0.59)	3.9 (0.06)	43.4 (0.69)
	200/13/135/60~80	20.9 (0.32)	66.7 (0.34)	3.6 (0.09)	40.8 (0.76)
	200/13/150/60~80	18.5 (0.21)	67.1 (0.57)	3.5 (0.05)	42.0 (0.67)
OD Treatment with MAPE	-	17.4 (0.34)	61.1 (0.91)	3.3 (0.12)	34.6 (1.05)
ICD Treatment without MAPE	200/11/120/60~80	16.9 (0.23)	56.5 (0.54)	2.9 (0.06)	33.5 (0.41)
OD Treatment without MAPE		14.2 (0.19)	48.9 (0.39)	2.6 (0.07)	27.9 (0.57)
*The results are given as averages and standard deviations (in parentheses) from the mean values					

The increase of air velocity, flexural strength, tensile strength, and modulus of elasticity of WPCs showed a trend of first increasing and then subsequent decreasing. This was because at a lower air volume, the fiber had longer retention in hot air, which caused more thermolysis in the fibers and the decomposition of hemicellulose and cellulose. The damages of the wood fibers resulted in decreased mechanical properties of WPCs. However, the fiber had a short retention in the hot air when the drying machine was operated at 13 m/s. Before a complete reaction, the hydroxide radicals in the fiber finished the heat treatment process, which caused a decrease of the mechanical properties. When the air velocity was over 10 m/s, the mechanical properties after ICD were all greater than those of the samples after OD. This indicated that there was a beneficial effect on impact strength, tensile strength, flexural strength, and modulus of elasticity of WPCs when a higher air velocity was used in ICD. For feed rate, the strength values of all WPC samples with ICD treatment were higher than those of the sample treated with the OD method. The results indicated that the ICD treatment improved the mechanical properties of WPCs. The mechanical properties of WPCs under the ICD treatment without MAPE were better than those of the OD treatment without MAPE. The flexural strength increased by 19.8%, the modulus of elasticity increased by 19.2%, the tensile strength was 21.5%, and the impact

strength increased by 23.2%. Under the high inlet temperature and inlet wind flow, the free hydroxyl reduction reduces the polarity of fibers and increases the dispersibility. However, the modification effect of drying without MAPE was still lower than those of drying treatment with MAPE.

Dispersibility Analysis

Figure 6 shows the dispersibility of wood fibers in WPCs after OD or ICD treatments. The results showed that the hydroxyl groups on the bridging part of wood fibers by OD were dehydrated to form a chemical bond, which made the wood fibers agglomerate. The distribution of ICD- treated fibers in the composite material was relatively loose. This occurred because the airflow of ICD did not cause agglomeration of the fibers, which effectively made the fibers in a well-dispersed state.

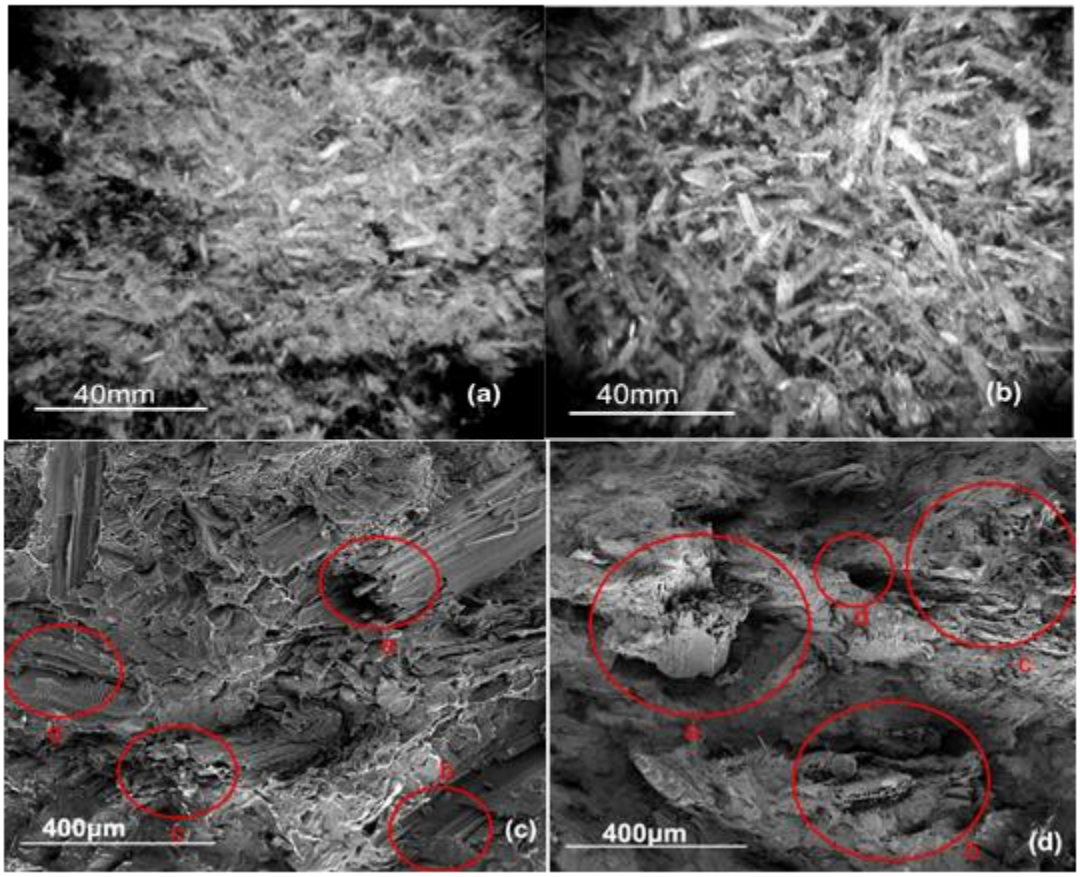

Fig. 6. Dispersibility of wood fibers with biological microscope and SEM: (a) Biological microscope of dispersibility of wood fibers by OD, (b) biological microscope of dispersibility of wood fibers by ICD under 200 °C /11 m/s/120 kg/h/60- to 80-meshes, (c) SEM of WPCs by OD, and (d) SEM of WPCs by ICD under 200 °C /11 m/s/120 kg/h /60- to 80-meshes

It was observed from the SEM of WPCs with the OD treatment that a large number of exposed fibers and partly agglomerated fibers were present on the impact-fractured surfaces. This suggested poor compatibility between the fiber and plastic, which led to the poor dispersion of wood fibers in the resin matrix and very low interaction between these two components. Figure 6(d) shows the SEM of WPCs by the ICD treatment. The results showed that the wood fibers were well wrapped by the plastic after ICD, which indicated that ICD improved dispersion and compatibility between the fiber and plastic matrix, and

further enhanced their interfacial binding in the composite material. Consequently, the material absorbed more energy under a continuous force with a clear enhancement of the mechanical properties, plasticity, and ductility of the composite material. Factors contributing to this improvement included the wood fiber in WPC containing some polar groups, such as alcoholic hydroxyl and phenolic hydroxyl groups. Furthermore, ICD decreased the number of alcoholic hydroxyl and phenolic hydroxyl groups, which improved the interfacial compatibility between the wood fiber and plastic, and consequently the mechanical properties of the composite material.

CONCLUSIONS

1. With the increase of the feed rate and the airflow, the final moisture content (MC) of the wood fibers showed an upward trend and the precipitation rate showed a negative trend.
2. The final MC displayed a downward trend and the precipitation rate exhibited an upward trend as the inlet temperature increased.
3. With the increase of the fiber mesh number, the final MC first increased and then decreased, while the precipitation rate first decreased and then increased.
4. The ICD-treated fibers had optimal dispersibility and stability during the mixing or compounding process. Selecting an appropriate drying treatment method was of significance for the performances of wood fibers and WPCs reinforced with fiber materials.
5. Compared with the oven drying method and the quality of the fibers treated by ICD, the composite material showed superior performances.
6. The FTIR results indicated that the number of hydroxyl and carbonyl groups was reduced greatly after ICD, which decreased the fiber polarity and resulted in better compatibility between the fiber and plastic matrix.
7. The ICD treatment changed the substances in the amorphous regions of the cellulose material. Thus, the crystallinity of poplar fiber with ICD increased from 46.6 to 67.0, which was higher than that with OD (40.8%).
8. Selecting an appropriate ICD with MAPE coupling agent method is of significance for the performances of wood fibers and WPCs reinforced with fiber materials. The mechanical properties of composite materials with ICD were better than those of oven -dried wood - plastic composites. Compared with ICD without MAPE, the composite material treated by ICD with MAPE showed superior performances.

ACKNOWLEDGMENTS

The authors gratefully acknowledge the financial support from the National Natural Science Foundation of China (Grant Nos. 31170529 and 31570550).

REFERENCES CITED

Akpinar, E., Midilli, A., and Bicer, Y. (2003). "Single layer drying behaviour of potato slices in a convective cyclone dryer and mathematical modeling," *Energy Conversion and Management* 44(10), 1689-1705. DOI: 10.1016/S0196-8904(02)00171-1

Butylina, S., Martikka, O., and Kärki, T. (2011). "Properties of wood fibre-polypropylene composites: Effect of wood fibre source," *Applied Composite Materials* 18(2), 101-111. DOI: 10.1007/s10443-010-9134-2

Dang, W., Song, Y., Wang, Q., and Wang, W. (2008). "Improvement in compatibility and mechanical properties of modified wood fiber/polypropylene composites," *Frontiers of Forestry in China* 3(2), 243-247. DOI: 10.1007/s11461-008-0021-z

Dev, S. R., and Raghavan, V. G. (2012). "Advancements in drying techniques for food, fiber, and fuel," *Drying Technology* 30(11-12), 1147-1159. DOI: 10.1080/07373937.2012.692747

Effah, B., Van Reenen, A., and Meincken, M. (2015). "Characterisation of the interfacial adhesion of the different components in wood-plastic composites with AFM," *Springer Science Reviews* 3(2), 97-111. DOI: 10.1007/s40362-015-0032-8

GB/T 1040 (1992). "Plastics – Determination of tensile properties," Standardization Administration of China, Beijing, China.

GB/T 1043 (1993). "Plastics – Determination of Charpy impact strength of rigid materials," Standardization Administration of China, Beijing, China.

GB/T 9341 (2000). "Plastics – Determination of flexural properties," Standardization Administration of China, Beijing, China.

GB/T 1931 (2009). "Method for determination of the moisture content of wood," Standardization Administration of China, Beijing, China.

Harper, D., and Wolcott, M. (2004). "Interaction between coupling agent and lubricants in wood–polypropylene composites," *Composites Part A: Applied Science and Manufacturing* 35(3), 385-394. DOI: 10.1016/j.compositesa.2003.09.018

Huang, S. H., Cortes, P., and Cantwell, W. J. (2006). "The influence of moisture on the mechanical properties of wood polymer composites," *Journal of Materials Science* 41(16), 5386-5390. DOI: 10.1007/s10853-006-0377-0

Jarusombuti, S., and Ayrilmis, N. (2011). "Surface characteristics and overlaying properti es of flat-pressed wood plastic composites," *European Journal of Wood and Wood Products* 69(3), 375-382. DOI: 10.1007/s00107-010-0440-z

Liu, M., Wang, J., Yan, J., Chong, D., and Liu, J. (2014). "A combined-type fluid-bed dryer suitable for integration within a lignite-fired power plant: System design and thermodynamic analysis," *Drying Technology* 32(8), 902-909. DOI: 10.1080/07373937.2013.875036

Ndiaye, D., Gueye, M., and Diop, B. (2013). "Characterization, physical, and mechanical properties of polypropylene/wood-flour composites," *Arabian Journal for Science and Engineering* 38(1), 59-68. DOI: 10.1007/s13369-012-0407-y

Pelaez-Samaniego, M. R., Yadama, V., Lowell, E., and Espinoza-Herrera, R. (2013). "A review of wood thermal pretreatments to improve wood composite properties," *Wood Science and Technology* 47(6), 1285-1319. DOI: 10.1007/s00226-013-0574-3

Ribeiro, H. A., and Costa, C. A. V. (2008). "A mechanical model for felt in impulse drying: A cellular materials approach. I. Model development and simulation," *Fibers and Polymers* 9(1), 55-62. DOI: 10.1007/s12221-008-0009-1

Sewda, K., and Maiti, S. N. (2013). "Dynamic mechanical properties of high density polyethylene and teak wood flour composites," *Polymer Bulletin* 70(10), 2657-2674. DOI: 10.1007/s00289-013-0941-0

Shi, J., Zhang, J., Pittman Jr., C. U., Toghiani, H., and Xue, Y. A. (2008). "Preliminary study of the stiffness enhancement of wood-plastic composites using carbon nanofibers," *Holz als Roh-und Werkstoff* 66(5), 313-322. DOI: 10.1007/s00107-008-0261-5

Wang, C., and Ying, S. (2014). "A novel strategy for the preparation of bamboo fiber rein forced polypropylene composites," *Fibers and Polymers* 15(1), 117-125. DOI: 10.1007/s12221-014-0117-z

Article submitted: November 22, 2016; Peer review completed: February 18, 2017; Revised version received and accepted: April 5, 2017; Published: April 14, 2017.
DOI: 10.15376/biores.12.2.3948-3964